Supplemental Material for "Higher-order topological insulators protected by (roto)inversion symmetries"

Guido van Miert[1] and Carmine Ortix[1,2]

[1] *Institute for Theoretical Physics, Center for Extreme Matter and Emergent Phenomena, Utrecht University, Princetonplein 5, 3584 CC Utrecht, Netherlands*
[2] *Dipartimento di Fisica "E. R. Caianiello", Universitá di Salerno, IT-84084 Fisciano, Italy*

(Dated: August 1, 2018)

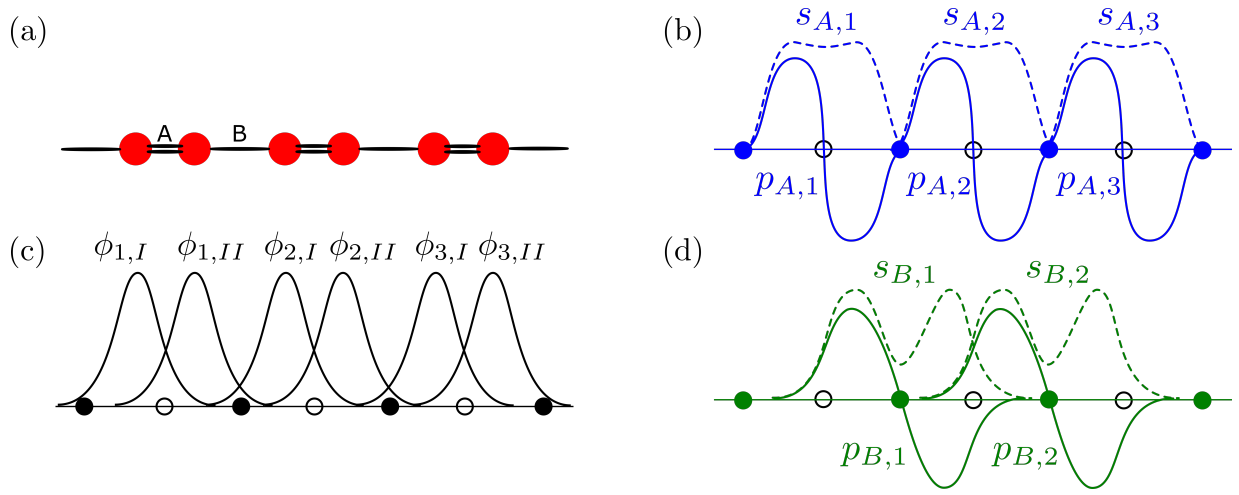

Figure 1. (a) Sketch of an Su-Schrieffer-Heeger chain. (b) Symmetry-adapted Wannier functions with respect to A. (c). Wannier functions centered at the atomic sites. (d) Symmetry-adapted Wannier functions with respect to B.

I. TOPOLOGY OF INVERSION-SYMMETRIC 1D CRYSTALS

In this section we discuss the topology of 1D inversion-symmetric crystals. We show that symmetry-adapted Wannier functions give rise to two topological $\mathbb{Z}$-invariants, and we will link these to the momentum space invariants.

Let us denote the Wannier functions for a one-dimensional inversion-symmetric chain in the compact form $w_{m;\alpha}(x) = w_\alpha(x-m)$, where α is the Wannier index while m is the unit-cell index (the lattice constant has been set to $a = 1$ for simplicity). The inversion symmetry of the chain implies the existence of two inversion centers within the unit cell, which, with a proper choice of the origin, can be fixed to $x = 0$ (Wyckoff position A) and $x = 1/2$ (Wyckoff position B).

For a symmetric Wannier function centered at the Wyckoff position A, the following transformation properties apply:

$$w_{m;\mu,A}(-x) \equiv \pm w_{-m;\mu,A}(x),$$

where $\pm$ refers to Wannier functions that are respectively even and odd under inversion, and we have explicitly split the Wannier index α into a site index and an orbital index μ. Symmetric Wannier functions centered at B instead transform as

$$w_{m;\mu,B}(-x) \equiv \pm w_{-m-1;\mu,B}(x).$$

These different transformation properties allow us to classify crystalline inversion-symmetric one-dimensional insulators with the set of four integers $N_{A(B);\pm1}$, *i.e.* the total number of occupied symmetric Wannier functions centered at $A(B)$ that are even and odd under inversion. As explained in the main text for $\mathcal{C}_4$ rotational-symmetric crystals, $N_{A(B);\pm1}$ do not represent genuine topological invariants.

Let us consider the Su-Schrieffer-Heeger model for spinless electrons [see Fig. 1(a),(b)] at integer filling. The ground state of this model can be expressed as a Slater determinant involving s-like and p-like orbitals centered at the inversion center A [c.f. Fig. 1(c)], whose Wannier functions we denote by $w_{m;s,A}(x)$ and $w_{m;p,A}(x)$ respectively. This implies that the associated set of integers defined above simply reads $N_{A;1} = N_{A;-1} = 1$, and $N_{B;1} = N_{B;-1} = 0$. However, this set of integers is not unique. In fact, starting out from the symmetric Wannier functions $w_{m;s/p,A}(x)$, it is possible to define new symmetric Wannier functions centered at B [c.f. Fig. 1](d) using the following relations

$$\begin{aligned} w_{m;s,B}(x) = \frac{1}{2}\,[&w_{m;s,A}(x) + w_{m+1;s,A}(x) + \\ &+ w_{m;p,A}(x) - w_{m+1;p,A}(x)] \\ w_{m;p,B}(x) = \frac{1}{2}\,[&-w_{m;s,A}(x) + w_{m+1;s,A}(x) \\ &- w_{m;p,A}(x) - w_{m+1;p,A}(x)] \end{aligned}$$

For these new Wannier functions, the set of integers clearly reads $N_{A;1} = N_{A;-1} = 0$ and $N_{B;1} = N_{B;-1} = 1$.

W	λ	Γ_1	Γ_{-1}	X_{-1}
A	1	1	0	0
	-1	0	1	1
B	1	1	0	1
	-1	0	1	0

Table I. Multiplicities at inversion-invariant momenta for symmetry adapted Wannier functions at Wyckoff position W with inversion eigenvalue λ.

The genuine topological invariants correspond to the difference between even and odd Wannier functions centered at the two Wyckoff positions, and thus read:

$$\nu_A = -N_{A;1} + N_{A;-1} \quad ; \quad \nu_B = -N_{B;1} + N_{B;-1}. \tag{1}$$

To prove that these integers are indeed topological invariants, we will now relate them to the symmetry labels in the band representation. We recall that the symmetry indicators of the band structure of a one-dimensional inversion-symmetric crystal correspond to the multiplicity of the even and odd eigenvalues of the inversion operator (with respect to inversion center A) at the BZ center $\Gamma = 0$, which we dub Γ_1 and Γ_{-1}, and at the BZ edge $X = \pi$, dubbed X_1 and X_{-1}. These symmetry labels are not independent since the existence of a band gap together with the continuity of the energy bands yields global constraints, known as compatibility relations, explicitly reading $\Gamma_1 + \Gamma_{-1} \equiv X_1 + X_{-1} \equiv N_F$, with N_F indicating the total number of occupied bands. To proceed further, we relate the two sets of integers stipulating the ansatz $\nu_{A(B)} = \gamma^{-1}_{A(B)}\Gamma_{-1} + \gamma^{1}_{A(B)}\Gamma_1 + x^{-1}_{A(B)}X_{-1}$, where we used that X_1 can be expressed in terms of the remaining symmetry labels via the compatibility relations. The linearity in the ansatz above is required by the fact that the topological invariant of two uncoupled systems must be additive. Next, we will determine the six unknowns $\gamma^{-1}_{A(B)}, \gamma^{1}_{A(B)}, x^{-1}_{A(B)}$ using the following constraints:

1. $\nu_{A(B)} = -1$, if we have a single even Wannier function centered a $A(B)$,

2. $\nu_{A(B)} = +1$, if we have a single odd Wannier function centered a $A(B)$,

3. $\nu_{A(B)} = 0$, if we have a single Wannier function centered at $B(A)$.

To do so, we analyze the inversion eigenvalues of the Bloch states $\psi_{q;\mu,\sigma}(x) = \sum_m e^{iqm} w_{m;\mu,\sigma}(x)$. Using the transformation properties of the symmetric Wannier functions, one finds

$$\begin{cases} \psi_{q;\mu,A}(-x) = \pm\, \psi_{-q;\mu,A}(x) \\ \\ \psi_{q;\mu,B}(-x) = \pm \mathrm{e}^{iq}\, \psi_{-q;\mu,A}(x), \end{cases}$$

where the plus (minus) sign refers to symmetric Wannier functions that are even (odd) under inversion. In Table I we list the inversion eigenvalues of the Bloch states corresponding to even and odd Wannier functions centered at the two Wyckoff positions. With this, the constraints listed above yield the following relations

$$\begin{cases} -1 = \gamma^1_A = \gamma^1_B + x^{-1}_B \\ 1 = \gamma^{-1}_A + x^{-1}_A = \gamma^{-1}_B \\ 0 = \gamma^1_A + x^{-1}_A = \gamma^{-1}_A = \gamma^{-1}_B + x^{-1}_B = \gamma^1_B, \end{cases}$$

which thereafter yield the expression for the topological invariants in terms of the inversion eigenvalues

$$\nu_A = \Gamma_{-1} - X_1 = -\Gamma_1 + X_{-1} \tag{2}$$
$$\nu_B = -\,\Gamma_1 + X_1 = \Gamma_{-1} - X_{-1} \tag{3}$$

All in all, the equations above serve a dual purpose: first they prove that $\nu_{A,B}$ are genuine topological invariants, since the inversion-symmetry eigenvalues can only change upon closing and reopening the band gap. Second, we have at hands an efficient strategy to bypass the problem of finding symmetry-adapted Wannier functions.

II. EDGE CHARGE OF INVERSION-SYMMETRIC 1D CRYSTALS

The 1D invariants ν_A and ν_B introduced above have a well-defined meaning. Let us consider a finite inversion-symmetric insulator in the atomic limit, with A as its center (the same considerations apply to B). Then, we find that the total number of states that is odd under inversion minus the total number of states that is even with respect to the center of the chain is precisely equal to ν_A. By invoking the principle of adiabatic continuity, we find that this statement holds in general.

Moreover, the $\mathbb{Z}_2$-part of ν_A pinpoints the value of the left and right edge charge, measured with respect to A: if ν_A is odd (even), there will be an odd (even) number of electrons on the chain, which implies that the left and right excess edge charge are semi-integer (integer), when measured with respect to A [see the main part of the manuscript]. Although this excess charge only probes the $\mathbb{Z}_2$-part, it is very robust in nature. Namely, even if the finite chain itself is not inversion-symmetric, as is typically the case, still the excess charges will be quantized for the very simple reason that charge cannot flow away from the edge as long as the bulk is insulating.

III. TOPOLOGY OF 2D ROTATION-SYMMETRIC CRYSTALS

In this section we discuss the topology of 2D rotation-symmetric crystals with zero Chern number. We provide a dictionary between the real-space topology expressed in terms of symmetry-adapted Wannier functions and the symmetry-labels in the band representation. We discuss in detail the topology of $\mathcal{C}_4$-symmetric crystals, after which we simply state the results for $\mathcal{C}_2$, $\mathcal{C}_3$, and $\mathcal{C}_6$-symmetric crystals.

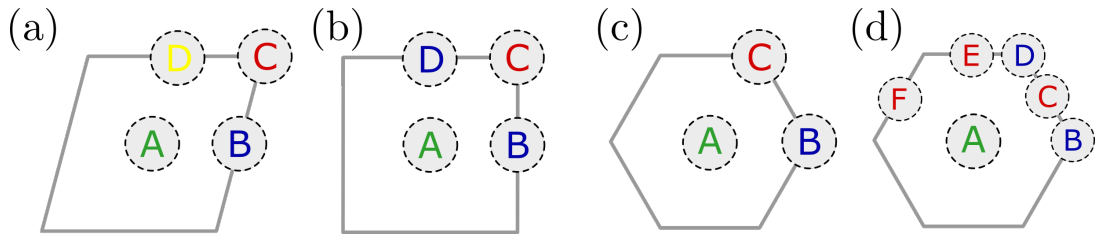

Figure 2. Wyckoff positions in rotation-symmetric crystals. (a) $\mathcal{C}_2$-symmetric crystal. (b) $\mathcal{C}_3$-symmetric crystal. (c) $\mathcal{C}_4$-symmetric crystal. (d) $\mathcal{C}_6$-symmetric crystal. Wyckoff positions related to each other by the rotation symmetry have the same color.

A. Integer crystalline topological invariants in $\mathcal{C}_4$-symmetric crystals

In a $\mathcal{C}_4$-symmetric crystal, there are two Wyckoff positions, A and C that are invariant under four-fold rotations, and two Wyckoff positions, B and D that are separately invariant under two-fold rotations, and transform into eachother under a fourfold rotation, see Fig. 2(b). The Wannier functions are symmetry-adapted if they satisfy the following transformation properties:

$$w_{\mathbf{m};\mu,A}(R\mathbf{x}) = r_{\mu,A} w_{R^{-1}\mathbf{m};\mu,A}(\mathbf{x}), \tag{4}$$
$$w_{\mathbf{m};\mu,C}(R\mathbf{x}) = r_{\mu,C} w_{R^{-1}\mathbf{m}-\mathbf{e}_2;\mu,C}(\mathbf{x}), \tag{5}$$
$$w_{\mathbf{m};\mu,B}(R\mathbf{x}) = r_{\mu,B/D} w_{R^{-1}\mathbf{m}-\mathbf{e}_2;\mu,D}(\mathbf{x}), \tag{6}$$
$$w_{\mathbf{m};\mu,D}(R\mathbf{x}) = w_{R^{-1}\mathbf{m};\mu,B}(\mathbf{x}). \tag{7}$$

where R denotes the rotation matrix, given by

$$R = \begin{pmatrix} 0 & -1 \\ 1 & 0 \end{pmatrix},$$

$\mathbf{e}_2 = (0,1)$, and the rotation eigenvalues satisfy $r^4_{\mu,A} = r^4_{\mu,C} = r^2_{\mu,B/D} = 1$. Note that this corresponds to a fourfold rotation around A. Given these Wannier functions we can define a set of integer $N_{A;1}, \ldots, N_{A;-i}, N_{C;1}, \ldots, N_{C;-i}, N_{B;1}$, $N_{B;-1}, N_{D;1}$, and $N_{D;-1}$ where $N_{A,\lambda}$ ($N_{C,\lambda}$) denotes the number of occupied fourfold symmetric Wannier functions centered at A (C) with rotation eigenvalue λ, and $N_{B(D),\lambda}$ denotes the number of occupied twofold symmetric Wannier

W	λ	Γ_1	Γ_i	Γ_{-1}	Γ_{-i}	M_i	M_{-1}	M_{-i}	X_{-1}
A	1	1	0	0	0	0	0	0	0
	i	0	1	0	0	1	0	0	1
	-1	0	0	1	0	0	1	0	0
	-i	0	0	0	1	0	0	1	1
C	1	1	0	0	0	0	1	0	1
	i	0	1	0	0	0	0	1	0
	-1	0	0	1	0	0	0	0	1
	-i	0	0	0	1	1	0	0	0
B+D	1	1	0	1	0	1	0	1	1
	-1	0	1	0	1	0	1	0	1

Table II. Multiplicities of the rotation eigenvalues at $\mathcal{C}_4$- and $\mathcal{C}_2$-invariant momenta for symmetry-adapted Wannier orbitals at Wyckoff position W and with rotation eigenvalue λ.

functions centered at B (D) with eigenvalue λ. Note that the fourfold rotational symmetry implies $N_{B;\pm1} = N_{D;\pm1}$. These integers, in turn, can be used to define the invariants $\nu_{A;\bar{r}}$, $\nu_{C;\bar{r}}$, and $\nu_B \equiv \nu_D$ defined in the main part of the manuscript.

We next make the following ansatz:

$$\begin{aligned}\nu_{W,\lambda} = {} & \gamma_1\Gamma_1 + \gamma_i\Gamma_i + \gamma_{-1}\Gamma_{-1} + \gamma_{-i}\Gamma_{-i} \\ & + m_iM_i + m_{-1}M_{-1} + m_{-i}M_{-i} + x_{-1}X_{-1}\end{aligned}$$

with $W = A, C, B$. Moreover, Γ_λ (M_λ) denotes the number of occupied bands at $\Gamma = (0,0)$ ($M = (\pi,\pi)$) with fourfold rotation eigenvalue λ, X_{-1} is the number of states at $X = (\pi, 0)$ that is odd under a twofold rotation, and γ_μ, m_μ, and x_μ are coefficients that we need to solve for. Let us shortly motivate this ansatz. Similarly to a one-dimensional atomic chain, we consider a function that is linear for the very simple reason that the numbers we have defined are additive. Second, we have not included the multiplicities X_1 and M_1, since we have used the following identity $\Gamma_1 + \Gamma_i + \Gamma_{-1} + \Gamma_{-i} = M_1 + M_i + M_{-1} + M_{-i} = X_1 + X_{-1}$, which corresponds to the compatibility relation for at two-fold rotational symmetric crystal. Third, we have not included the multiplicities at Y since these are identical to the multiplicities at X. In Table II we list the multiplicities of the rotation eigenvalues for a single symmetry-adapted Wannier function centered at one of the four Wyckoff positions. These values have been obtained by Fourier transforming Eqs. (4)-(7). Using these values, we can solve for the eight unknowns of each integer topological invariant. We find the following relations:

$$\begin{aligned}
\nu_{A;1} &= -3\Gamma_1 - \frac{3}{2}\Gamma_i - \Gamma_{-1} - \frac{3}{2}\Gamma_{-i} + \frac{3}{2}M_i + 2M_{-1} + \frac{3}{2}M_{-i} + X_{-1}, \\
\nu_{A;i} &= \Gamma_1 - \frac{1}{2}\Gamma_i + \Gamma_{-1} + \frac{3}{2}\Gamma_{-i} - \frac{3}{2}M_i + \frac{1}{2}M_{-1} - X_{-1}, \\
\nu_{A;-1} &= \Gamma_1 + \frac{1}{2}\Gamma_i - \Gamma_{-1} + \frac{1}{2}\Gamma_{-i} - \frac{1}{2}M_i - 2M_{-1} - \frac{1}{2}M_{-1} + X_{-1}, \\
\nu_{C;1} &= \frac{3}{2}\Gamma_i + 2\Gamma_{-1} + \frac{3}{2}\Gamma_{-i} - \frac{1}{2}M_i - 2M_{-1} - \frac{1}{2}M_{-i} - X_{-1}, \\
\nu_{C;i} &= -\frac{3}{2}\Gamma_i + \frac{1}{2}\Gamma_{-i} + \frac{1}{2}M_i - \frac{3}{2}M_{-i} + X_{-1}, \\
\nu_{C;-1} &= -\frac{1}{2}\Gamma_i - 2\Gamma_{-1} - \frac{1}{2}\Gamma_{-i} + \frac{3}{2}M_i + 2M_{-1} + \frac{3}{2}M_{-i} - X_{-1}, \\
\nu_B &= \frac{1}{2}\Gamma_i + \frac{1}{2}\Gamma_{-i} - \frac{1}{2}M_i - \frac{1}{2}M_{-i}.
\end{aligned}$$

B. Integer crystalline topological invariants in $\mathcal{C}_2$-symmetric crystals

In a 2D $\mathcal{C}_2$-symmetric crystal we find four $\mathcal{C}_2$-symmetric Wyckoff positions per unit cell. These are labeled as A, B, C, and D, see Fig. 2(a). The Wannier functions are symmetry-adapted if they satisfy the following properties:

$$w_{\mathbf{m};\mu,A}(-\mathbf{x}) = r_{\mu,A} w_{-\mathbf{m};\mu,A}(\mathbf{x}), \tag{8}$$
$$w_{\mathbf{m};\mu,B}(-\mathbf{x}) = r_{\mu,B} w_{-\mathbf{m}-\mathbf{e}_1;\mu,B}(\mathbf{x}), \tag{9}$$
$$w_{\mathbf{m};\mu,C}(-\mathbf{x}) = r_{\mu,C} w_{-\mathbf{m}-\mathbf{e}_1-\mathbf{e}_2;\mu,C}(\mathbf{x}), \tag{10}$$
$$w_{\mathbf{m};\mu,D}(-\mathbf{x}) = r_{\mu,D} w_{-\mathbf{m}-\mathbf{e}_2;\mu,D}(\mathbf{x}), \tag{11}$$

where $\mathbf{e}_1 = (1,0)$ and the rotation eigenvalues satisfy $r^2_{\mu,A} = r^2_{\mu,B} = r^2_{\mu,C} = r^2_{\mu,D} = 1$. Given these Wannier functions, let $N_{W;\pm1}$ denote the number of occupied two-fold rotation symmetric Wannier functions centered at W with rotation eigenvalue ±1. Out of these eight integers we can extract four $\mathbb{Z}$ invariants given by

$$\begin{aligned}
\nu_A &= -N_{A;1} + N_{A;-1}, \\
\nu_B &= -N_{B;1} + N_{B;-1}, \\
\nu_C &= -N_{C;1} + N_{C;-1}, \\
\nu_D &= -N_{D;1} + N_{D;-1}.
\end{aligned}$$

We now follow the strategy laid out in the main text and in Secs. I and III.A to show that these are indeed proper invariants. Therefore, we relate them to the band structure multiplicities $\Gamma_{\pm1}$, X_{-1}, Y_{-1}, and M_{-1}. We simply state the results:

$$\begin{aligned}
\nu_A &= -\Gamma_1 - \frac{1}{2}\Gamma_{-1} + \frac{1}{2}X_{-1} + \frac{1}{2}Y_{-1} + \frac{1}{2}M_{-1}, \\
\nu_B &= \frac{1}{2}\Gamma_{-1} - \frac{1}{2}X_{-1} + \frac{1}{2}Y_{-1} - \frac{1}{2}M_{-1}, \\
\nu_C &= \frac{1}{2}\Gamma_{-1} - \frac{1}{2}X_{-1} - \frac{1}{2}Y_{-1} + \frac{1}{2}M_{-1}, \\
\nu_D &= \frac{1}{2}\Gamma_{-1} + \frac{1}{2}X_{-1} - \frac{1}{2}Y_{-1} - \frac{1}{2}M_{-1}.
\end{aligned}$$

These results have been obtained by using the multiplicities of the rotation eigenvalues for single symmetry-adapted Wannier functions centered at one of the Wyckoff positions, see Table III.

W	λ	Γ_1	Γ_{-1}	X_{-1}	Y_{-1}	M_{-1}
A	1	1	0	0	0	0
	-1	0	1	1	1	1
B	1	1	0	1	0	1
	-1	0	1	0	1	0
C	1	1	0	1	1	0
	-1	0	1	0	0	1
D	1	1	0	0	1	1
	-1	0	1	1	0	0

Table III. Multiplicities of the rotation eigenvalues at $\mathcal{C}_2$-invariant momenta for symmetry-adapted Wannier functions at Wyckoff position W and with rotation eigenvalue λ.

C. Integer crystalline topological invariants in $\mathcal{C}_3$-symmetric crystals

In a 2D $\mathcal{C}_3$-symmetric crystal we find three $\mathcal{C}_3$-symmetric Wyckoff positions per unit cell. These are labeled as A, B, and C, , see Fig. 2(c). As before, we assume to have found symmetry-adapted Wannier functions, and let $N_{A;\lambda}$, $N_{B;\lambda}$, and$N_{C;\lambda}$ denote the total number of occupied symmetry-adapted Wannier functions at A, B, and C, with three-fold

rotation eigenvalue λ. To ensure immunity against continuous deformations of the type shown in Fig. 1(b) in the main text, which correspond to $N_{W;\lambda} \to N_{W;\lambda} \pm 1 \forall \lambda$, we are led to define a new set of six integers:

$$\nu_{W;\bar{r}} = -2N_{W;\bar{r}} + \sum_{r \neq \bar{r}} N_{W;r} \;\; \bar{r} = 1, e^{i2\pi/3} \;;\; W = A, B, C.$$

As before, we can express these in terms of the multiplicities $\Gamma_{\bar{r}}$, $K^+_{\bar{r}}$, and $K^-_{\bar{r}}$ of the threefold rotation eigenvalues $\bar{r}$ at the high-symmetry points Γ, K^+, and K^-. These relations read:

$$\begin{aligned}
\nu_{A,1} &= -2\Gamma_1 - \Gamma_{e^{i2\pi/3}} - \Gamma_{e^{i4\pi/3}} + K^+_{e^{i2\pi/3}} + K^+_{e^{i4\pi/3}} \\
&\quad + K^-_{e^{i2\pi/3}} + K^-_{e^{i4\pi/3}}, \\
\nu_{A,e^{i2\pi/3}} &= \Gamma_1 + \Gamma_{e^{i4\pi/3}} - K^+_{e^{i2\pi/3}} - K^-_{e^{i2\pi/3}}, \\
\nu_{B,1} &= \Gamma_{e^{i2\pi/3}} + \Gamma_{e^{i4\pi/3}} - K^+_{e^{i2\pi/3}} - K^-_{e^{i4\pi/3}}, \\
\nu_{B,e^{i2\pi/3}} &= -\Gamma_{e^{i2\pi/3}} - K^+_{e^{i4\pi/3}} + K^-_{e^{i2\pi/3}} + K^-_{e^{i4\pi/3}}, \\
\nu_{C,1} &= \Gamma_{e^{i2\pi/3}} + \Gamma_{e^{i4\pi/3}} - K^+_{e^{i4\pi/3}} - K^-_{e^{i2\pi/3}}, \\
\nu_{C,e^{i2\pi/3}} &= -\Gamma_{e^{i2\pi/3}} + K^+_{e^{i2\pi/3}} + K^+_{e^{i4\pi/3}} - K^-_{e^{i4\pi/3}}.
\end{aligned}$$

These formulas have been obtained by considering the multiplicities of the rotation eigenvalues for a single symmetry-adapted Wannier function centered at one of the Wyckoff positions, see Table IV.

W	λ	Γ_1	$\Gamma_{e^{i\frac{2\pi}{3}}}$	$\Gamma_{e^{i\frac{2\pi}{3}}}$	$K^+_{e^{i\frac{2\pi}{3}}}$	$K^+_{e^{i\frac{2\pi}{3}}}$	$K^-_{e^{i\frac{2\pi}{3}}}$	$K^-_{e^{i\frac{2\pi}{3}}}$
A	1	1	0	0	0	0	0	0
	$e^{i\frac{2\pi}{3}}$	0	1	0	1	0	1	0
	$e^{i\frac{4\pi}{3}}$	0	0	1	0	1	0	1
B	1	1	0	0	1	0	0	1
	$e^{i\frac{2\pi}{3}}$	0	1	0	0	1	0	0
	$e^{i\frac{4\pi}{3}}$	0	0	1	0	0	1	0
C	1	1	0	0	0	1	1	0
	$e^{i\frac{2\pi}{3}}$	0	1	0	0	0	0	1
	$e^{i\frac{4\pi}{3}}$	0	0	1	1	0	0	0

Table IV. Multiplicities of the rotation eignevalues at $\mathcal{C}_3$-invariant momenta for symmetry-adapted Wannier functions at Wyckoff position W and with rotation eigenvalue λ.

D. Integer crystalline topological invariants in $\mathcal{C}_6$-symmetric crystals

In a $\mathcal{C}_6$-symmetric crystal, each unit cell hosts a single six-fold invariant Wyckoff position A, two three-fold invariant positions B and D, and three two-fold invariant points C, E, and F, see Fig. 2(d). However, since all three- and two-fold positions are related by the six-fold symmetry, we only have two provide the number of symmetry-adapted Wannier functions at A, B, and C. As before, we require that the invariants are immune to transformations of the type shown in Fig. 1(b) in the main text. Hence, we find the following invariants:

$$\begin{aligned}
\nu_{A;\bar{r}} &= -5N_{A;\bar{r}} + \sum_{r \neq \bar{r}} N_{A;r} \;\; \bar{r} = 1, e^{i\pi/3}, e^{i2\pi/3}, -1, e^{i4\pi/3}, \\
\nu_{B;\bar{r}} &= -2N_{B;\bar{r}} + \sum_{r \neq \bar{r}} N_{B;r} \;\; \bar{r} = 1, e^{i2\pi/3}, \\
\nu_{C;1} &= -N_{C;1} + N_{C;-1}.
\end{aligned}$$

W	λ	Γ_1	$\Gamma_{e^{i\frac{\pi}{3}}}$	$\Gamma_{e^{i\frac{2\pi}{3}}}$	Γ_{-1}	$\Gamma_{e^{i\frac{4\pi}{3}}}$	$\Gamma_{e^{i\frac{5\pi}{3}}}$	M_{-1}	$K_{e^{i\frac{2\pi}{3}}}$	$K_{e^{i\frac{4\pi}{3}}}$
A	1	1	0	0	0	0	0	0	0	0
	$e^{i\frac{\pi}{3}}$	0	1	0	0	0	0	1	1	0
	$e^{i\frac{2\pi}{3}}$	0	0	1	0	0	0	0	0	1
	-1	0	0	0	1	0	0	1	0	0
	$e^{i\frac{4\pi}{3}}$	0	0	0	0	1	0	0	1	0
	$e^{i\frac{5\pi}{3}}$	0	0	0	0	0	1	1	0	1
B+D	1	1	0	0	1	0	0	1	1	1
	$e^{i\frac{2\pi}{3}}$	0	1	0	0	1	0	1	0	1
	$e^{i\frac{4\pi}{3}}$	0	0	1	0	0	1	1	1	0
C+E+F	1	1	0	1	0	1	0	2	1	1
	-1	0	1	0	1	0	1	1	1	1

Table V. Multiplicities of the rotation eigenvalues at C_6-invariant momenta for symmetry-adapted Wannier functions at Wyckoff position W and with rotation eigenvalue λ.

Expressed in terms of the multiplicities of the rotation eigenvalues at high-symmetry points, we find:

$$\begin{aligned}
\nu_{A;1} &= -5\Gamma_1 - \frac{5}{2}\Gamma_{e^{i\pi/3}} - \Gamma_{e^{i2\pi/3}} - \frac{1}{2}\Gamma_{-1} - \Gamma_{e^{i4\pi/3}} - \frac{5}{2}\Gamma_{e^{i5\pi/3}} + 2K^+_{e^{i2\pi/3}} + 2K^+_{e^{i4\pi/3}} + \frac{3}{2}M_{-1},\\
\nu_{A;e^{i\pi/3}} &= \Gamma_1 - \frac{3}{2}\Gamma_{e^{i\pi/3}} + \Gamma_{e^{i2\pi/3}} + \frac{5}{2}\Gamma_{-1} + 3\Gamma_{e^{i4\pi/3}} - 2K^+_{e^{i2\pi/3}} - \frac{3}{2}M_{-1},\\
\nu_{A;e^{i2\pi/3}} &= \Gamma_1 - \frac{1}{2}\Gamma_{e^{i\pi/3}} - 3\Gamma_{e^{i2\pi/3}} - \frac{1}{2}\Gamma_{-1} + \Gamma_{e^{i4\pi/3}} - 2K^+_{e^{i4\pi/3}} + \frac{3}{2}M_{-1},\\
\nu_{A;-1} &= \Gamma_1 + \frac{1}{2}\Gamma_{e^{i\pi/3}} - \Gamma_{e^{i2\pi/3}} - \frac{7}{2}\Gamma_{-1} - \Gamma_{e^{i4\pi/3}} + 2K^+_{e^{i2\pi/3}} + 2K^+_{e^{i4\pi/3}} - \frac{3}{2}M_{-1},\\
\nu_{A;e^{i4\pi/3}} &= \Gamma_1 + \frac{3}{2}\Gamma_{e^{i\pi/3}} + \Gamma_{e^{i2\pi/3}} - \frac{1}{2}\Gamma_{-1} - 3\Gamma_{e^{i4\pi/3}} - 2K^+_{e^{i2\pi/3}} + \frac{3}{2}M_{-1},\\
\nu_{B;1} &= \Gamma_{e^{i\pi/3}} + \Gamma_{e^{i2\pi/3}} + \Gamma_{e^{i4\pi/3}} - K^+_{e^{i2\pi/3}} - K^+_{e^{i4\pi/3}},\\
\nu_{B;e^{i2\pi/3}} &= -\Gamma_{e^{i\pi/3}} - \Gamma_{e^{i4\pi/3}} + K^+_{e^{i2\pi/3}},\\
\nu_{C;1} &= \frac{1}{2}\Gamma_{e^{i\pi/3}} + \frac{1}{2}\Gamma_{-1} - \frac{1}{2}M_{-1}.
\end{aligned}$$

As before, these formulas have been obtained by considering the multiplicities of the rotation eigenvalues for single symmetry-adapted Wannier functions centered at one of the Wyckoff positions, see Table V.

E. Integer crystalline topological invariants in $\mathcal{C}_n\mathcal{M}_z$-symmetric crystals, with $n = 2, 4,$ and 6.

Although, the analysis presented in Sec. III applies to $\mathcal{C}_n$-symmetric crystals, however, essentially the same invariants characterize the symmetry-adapted Wannier functions in crystals that are $\mathcal{C}_n\mathcal{M}_z$-symmetric, with $n = 2, 4,$ and 6 and $\mathcal{M}_z$ the out-of-plane reflection symmetry.

IV. CORNER CHARGE OF ROTATION-SYMMETRIC 2D CRYSTALS

For 1D inversion-symmetric insulators we have shown that the $\mathbb{Z}_2$ part of the invariants ν_A and ν_B can be related to the edge charges. Now suppose we consider a 2D crystalline insulator with a $\mathcal{C}_n$-symmetric bulk. Let ν_A denote the $\mathbb{Z}_m$ part of an invariant associated with a Wyckoff position A. Now in general, if A is invariant under an m-fold rotation, then the corner charge, measured with respect to A, is given by ν_A/m. Indeed, we have explicitly shown this in the main text for a $\mathcal{C}_4$-symmetric crystal with A a $\mathcal{C}_4$-invariant Wyckoff position. The same reasoning, applies to $\mathcal{C}_3$ and $\mathcal{C}_6$-symmetric corners. As stressed in the main text, it is crucial that the two edges that intersect at the corner are related by the same m-fold rotational symmetry. This is also illustrated schematically in Fig. 3(b), (c), and (d). Special care has to be taken if $m = 2$, since two edges related by $\mathcal{C}_2$ do not intersect each-other. In this

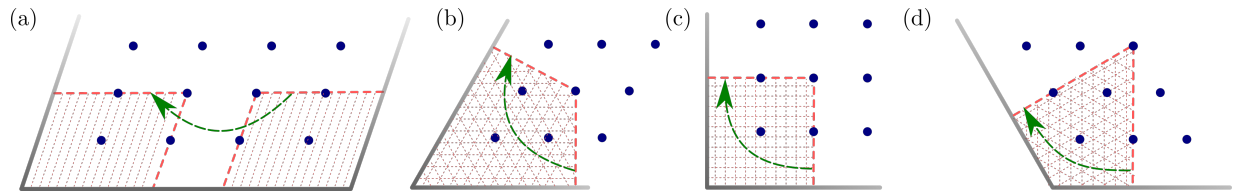

Figure 3. Corners with edges related by $\mathcal{C}_m$-symmetry. The blue dots denote Wyckoff positions A. The charge inside the dashed region is then given by ν_A/m. (a) corresponds to $m = 2$, (b) $m = 3$, (c) $m = 4$, and (d) $m = 6$.

case, one should consider the sum of the lower-left corner charge and lower-right corner charge, both measured with respect to the same two-fold symmetric Wyckoff position A, see Fig. 3(a).

V. CORNER CHARGE PUMPS AND CHIRAL HINGE STATES

Let us consider a 3D $\mathcal{S}_n = \mathcal{C}_n\mathcal{M}_z$-symmetric insulator, with $n = 2, 4$, or 6. Here, $\mathcal{S}_2$ is simply inversion, $\mathcal{S}_4$ a four-fold roto-inversion, while $\mathcal{S}_6$ corresponds to a three-fold roto-inversion, which therefore is both inversion and three-fold rotationally symmetric. Such a 3D crystal can be seen as a collection of 2D systems with Hamiltonians $\mathcal{H}(k_z)$ parametrized by k_z. In particular, for $k_z = 0, \pi$ we find that the 2D Hamiltonian is $\mathcal{S}_n$-symmetric. Now let us consider a geometry with surfaces that are related by the (roto)-inversion symmetry. Then, we find that the corner charge $Q_A(k_z)$, with A a Wyckoff position invariant under $\mathcal{S}_n$, satisfies the following relation:

$$Q_A(k_z) = -Q_A(-k_z) \bmod \frac{2}{n}.$$

This formula follows from the following observations: *(i)* The total charge in the edge and bulk parts is integer, which implies that the sum of all corner charges is integer. *(ii)* The corner charges at two-neighboring corners at $+k_z$ and $-k_z$ are identical, see also Fig. 4. *(iii)* The corner charges at corners related by $\mathcal{S}_n^2$ are identical (since this operation leaves k_z untouched).

Now imagine that $Q_A(\pi) - Q_A(0) = 1/2(0) \bmod 1$. Then, each hinge sandwiched between two surfaces related by the $\mathcal{S}_n$-symmetry will host an odd (even) number of chiral states. Since $Q_A(0)$ and $Q_A(\pi)$ are given by $\nu_A(0)/n$ and $\nu_A(\pi)/n$, respectively, this translates into the statement that if and only if $\nu_A(\pi) - \nu_A(0) = n/2 \bmod 1$, then the system is a non-trivial higher order topological insulator. Note, that for an $\mathcal{S}_2$-symmetric, insulator, two hinges are sandwiched between two surfaces related by the $\mathcal{S}_2$-symmetry. The invariant does not pinpoint on which of these two hinges the chiral state will reside: This is simply a microscopic detail of the specific surface.

Finally, we illustrate these finding for a $\mathcal{S}_6$-symmetric toy model. First, we consider the 2D honeycomb lattice with a Kekule distortion, such that the unit-cell hosts six sites, see Fig. 5(a). The intra(inter)-unit cell hopping is given by t_1 (t_2). In the flat band limit, with $t_1 \neq 0$ and $t_2 = 0$, we find that at half-filling the energies of the bands are given by

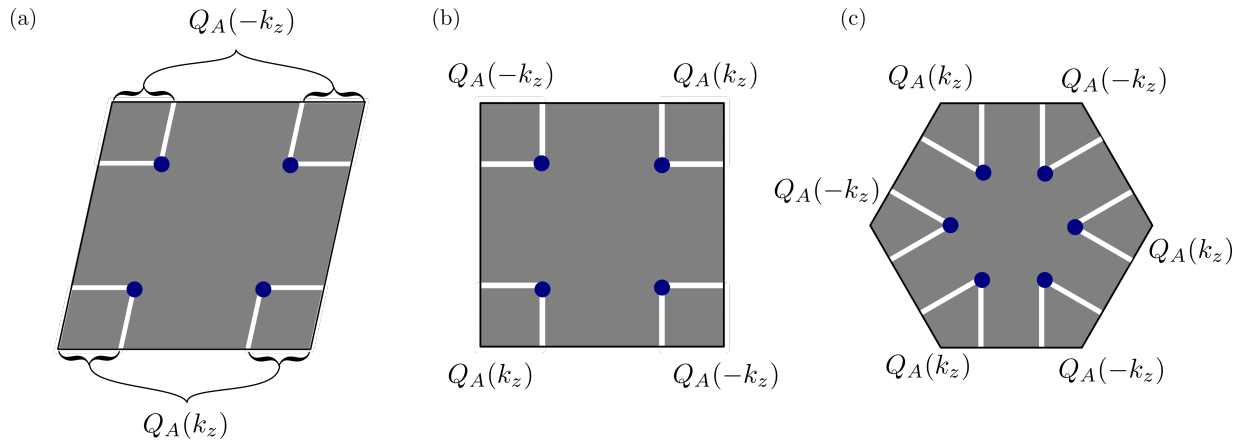

Figure 4. Corner charge $Q_A(k_z)$ with respect to Wyckoff position A, shown in blue, for a given k_z. (a), (b), and (c) correspond to $\mathcal{S}_2$, $\mathcal{S}_4$, and $\mathcal{S}_6$, respectively.

$\pm 2t_1, \pm t_1$, with the latter doubly degenerate. Moreover, the topological invariant reads $\nu_A = 3 \bmod 6$, and all others are zero. Similarly, we can consider the opposite limit, $t_1 = 0$, and $t_2 \neq 0$. Then, the bands are triply degenerate, and have energies $\pm t_2$. Moreover, at half-filling we find $\nu_C = 1 \bmod 2$, whereas all other invariants are zero. So in the latter case we expect that the corner charge measured with respect to A vanishes, whereas in the former case, we expect that the corner charge is precisely equal to one half of the electron's charge.

Next, let us consider a three-dimensional extension of this model. Here, we consider a 3D stack of the 2D lattices. We connect the stacks through purely imaginary nearest-neighbor hoppings $\pm i t_3$, as well as real diagonal next-nearest neighbor hoppings t_4, see Fig. 5(b). These interlayer hopping break the $\mathcal{C}_6$ and $\mathcal{M}_z$ symmetries, but respect their combination $\mathcal{S}_6$. The Hamiltonian reads

$$\mathcal{H}_{\mathbf{k}} = - \begin{pmatrix} 2t_3 \sin(\mathbf{k}\cdot\mathbf{a}_3) & t_1 + t_4 e^{i\mathbf{k}\cdot\mathbf{a}_3} & 0 & t_2 e^{i\mathbf{k}\cdot(\mathbf{a}_1-\mathbf{a}_2)} & 0 & t_1 + t_4 e^{i\mathbf{k}\cdot\mathbf{a}_3} \\ t_1 + t_4 e^{-i\mathbf{k}\cdot\mathbf{a}_3} & -2t_3 \sin(\mathbf{k}\cdot\mathbf{b}_3) & t_1 + t_4 e^{-i\mathbf{k}\cdot\mathbf{a}_3} & 0 & t_2 e^{i\mathbf{k}\cdot\mathbf{a}_1} & 0 \\ 0 & t_1 + t_4 e^{i\mathbf{k}\cdot\mathbf{a}_3} & 2t_3 \sin(\mathbf{k}\cdot\mathbf{a}_3) & t_1 + t_4 e^{i\mathbf{k}\cdot\mathbf{a}_3} & 0 & t_2 e^{i\mathbf{k}\cdot\mathbf{a}_2} \\ t_2 e^{-i\mathbf{k}\cdot(\mathbf{a}_1-\mathbf{a}_2)} & 0 & t_1 + t_4 e^{-i\mathbf{k}\cdot\mathbf{a}_3} & -2t_3 \sin(\mathbf{k}\cdot\mathbf{a}_3) & t_1 + t_4 e^{-i\mathbf{k}\cdot\mathbf{a}_3} & 0 \\ 0 & t_2 e^{-i\mathbf{k}\cdot\mathbf{a}_1} & 0 & t_1 + t_4 e^{i\mathbf{k}\cdot\mathbf{a}_3} & 2t_3 \sin(\mathbf{k}\cdot\mathbf{a}_3) & t_1 + t_4 e^{i\mathbf{k}\cdot\mathbf{a}_3} \\ t_1 + t_4 e^{-i\mathbf{k}\cdot\mathbf{a}_3} & 0 & t_2 e^{-i\mathbf{k}\cdot\mathbf{a}_2} & 0 & t_1 + t_4 e^{-i\mathbf{k}\cdot\mathbf{a}_3} & -2t_3 \sin(\mathbf{k}\cdot\mathbf{a}_3) \end{pmatrix}.$$

In Fig. 5(c) we plot the bulk band structure along HS lines, for $t_1 = 1$, $t_2 = 1.2$, $t_3 = .8$, and $t_4 = .9$. For these parameters, we find that in the $k_z = 0$ plane, the invariant $\nu_A = 3 \bmod 6$, and for $k_z = 0$, we find $\nu_A = 0 \bmod 6$. Hence, we expect the presence of chiral hinge states for a geometry of the type shown in Fig. 4(c). This is indeed the case, see Fig. 5(d), where we plot the corresponding band structure with periodic boundary conditions in the z direction.

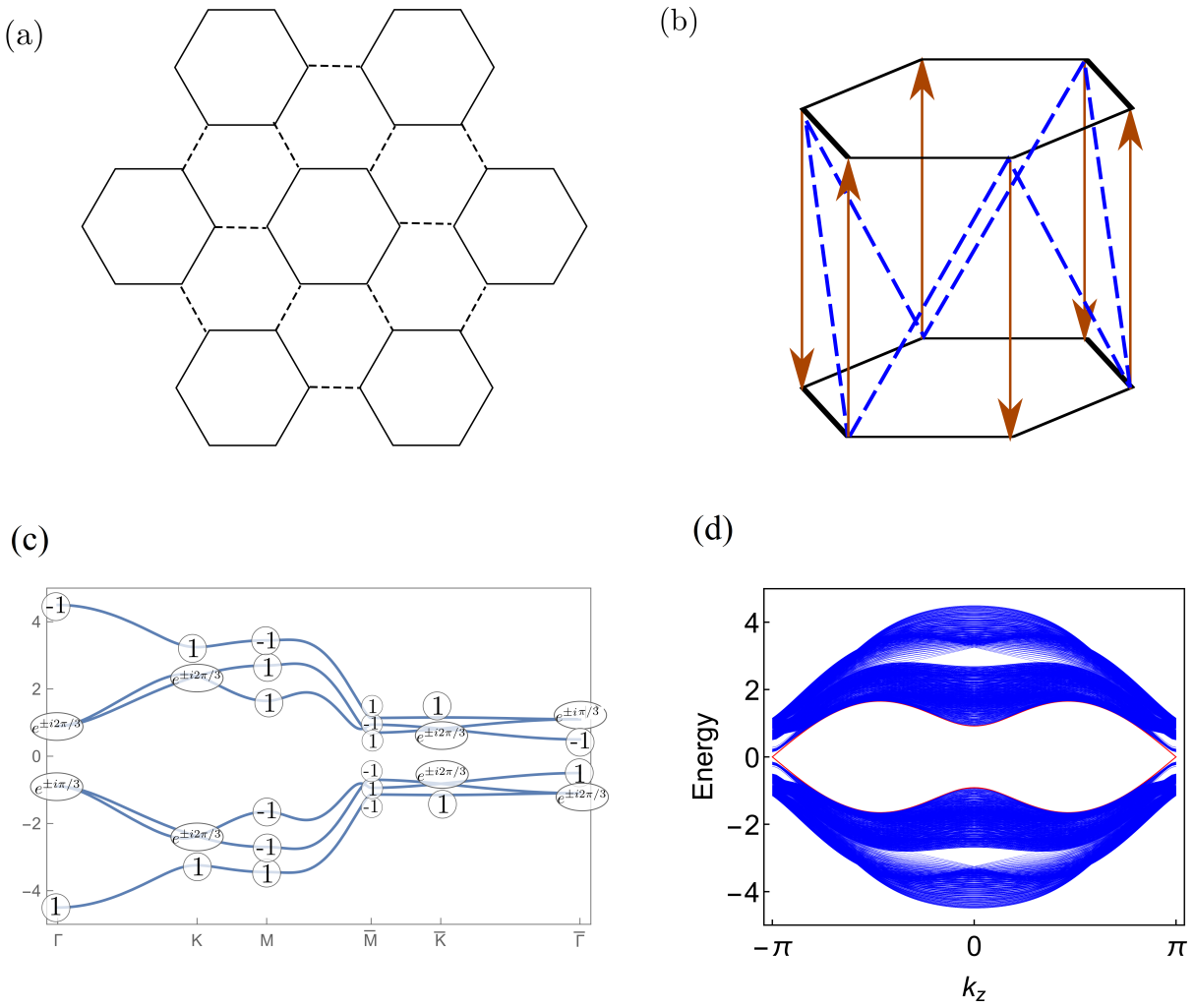

Figure 5. (a) $\mathcal{C}_6$-symmetric Kekule distortion in graphene. Solid (dashed) lines correspond to intra (inter) unit cell hopping parameters t_1 (t_2). (b) Sketch of interlayer hopping parameters for a 3D higher-order topological insulator. Dashed lines corresponds to t_4, while the arrows correspond to $\pm it_3$. Both break $\mathcal{C}_6$ and $\mathcal{M}_z$ individually, but respect their combination. The purely imaginary hopping parameters $\pm it_3$ break time-reversal symmetry. (c) Bulk band structure along high-symmetry lines, with rotation eigenvalues at high-symmetry momenta. (d) Corresponding band structure for a system with periodic boundary conditions in the $\hat{z}$-direction, while open in the other directions.